Arxiv: 2406.05178

The Star-Forming Main Sequence in JADES and CEERS at $z > 1.4$: Investigating the Burstiness of Star Formation

Leonardo Clarke [1], Alice E. Shapley [1], Ryan L. Sanders [2,*], Michael W. Topping [3], Gabriel B. Brammer [4,5], Trinity Bento,[1] Naveen A. Reddy [6] and Emily Kehoe[1]

ABSTRACT

We have used public JWST/NIRSpec and JWST/NIRCam observations from the CEERS and JADES surveys in order to analyze the star-forming main sequence (SFMS) over the redshift range $1.4 \leq z < 7$. We calculate the star-formation rates (SFRs) of the galaxy sample using three approaches: Balmer line luminosity, spectral energy distribution (SED) fitting, and UV luminosity. We find a larger degree of scatter about the SFMS using the Balmer-based SFRs compared to the UV-based SFRs. Because these SFR indicators are sensitive to star formation on different time scales, the difference in scatter may be evidence of bursty star-formation histories in the early universe. We additionally compare the Hα-to-UV luminosity ratio ($L(H\alpha)/\nu L_{\nu,1600}$) for individual galaxies in the sample and find that 29%−52% of the ratios across the sample are poorly described by predictions from a smooth star-formation history. Measuring the burstiness of star formation in the early universe has multiple significant implications, such as deriving accurate physical parameters from SED fitting, explaining the evolution of the UV luminosity function, and providing constraints for sub-grid models of feedback in simulations of galaxy formation and evolution.

Introduction:

SFMS: galaxies are experiencing a smooth buildup of stellar mass over time
The intrinsic scatter in the SFMS → "burstiness" of galaxy SFHs
Bursty SFHs may cause the excess of galaxies at the bright end of the UV LF

Observations and Measurements:

CEERS + JADES
SED: FAST (FSPS + delayed-τ + sub-solar metallicity + SMC curve)

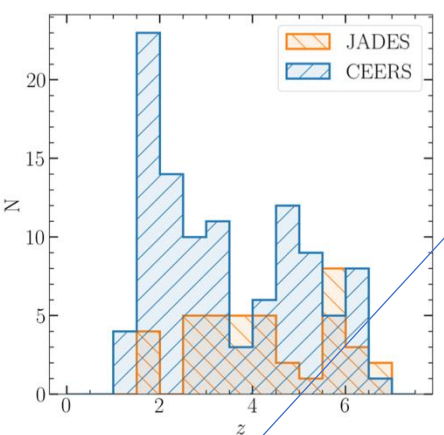

Sample selection criteria:
1) JWST/NIRCam + 3DHST photometry
2) >5σ detections of at least two Balmer lines for dust correction
3) log (sSFR(SED)/yr) > −11
4) Remove AGN contamination [N II]/Hα flux ratio < 0.5
→ 146 galaxies in the redshift range $1.4 \leq z < 7$

Figure 1. Redshift distribution of the combined CEERS and JADES sample that we analyze consisting of 146 spectroscopically confirmed star-forming galaxies with robust SED measurements. Of these, 106 galaxies come from CEERS and 40 galaxies come from JADES.

SFR indicators:
1) dust-corrected Hα luminosity
2) the SED-based SFR from FAST
3) dust-corrected UV luminosity

$$\log\left(\frac{\mathrm{SFR}}{\mathrm{M_\odot\ yr^{-1}}}\right) = \log\left(\frac{\mathrm{L_{H\alpha}}}{\mathrm{erg\ s^{-1}}}\right) + C \quad C = -41.59$$

$$\log\left(\frac{\mathrm{SFR}}{\mathrm{M_\odot\ yr^{-1}}}\right) = \log\left(\frac{\nu \mathrm{L}_{\nu,1600}}{\mathrm{erg\ s^{-1}}}\right) - 43.35$$

Five redshift bins: $1.4 < z \leq 2.7$, $2.7 < z \leq 4$, $4 < z \leq 5$, $5 < z \leq 6$, $6 < z \leq 7$

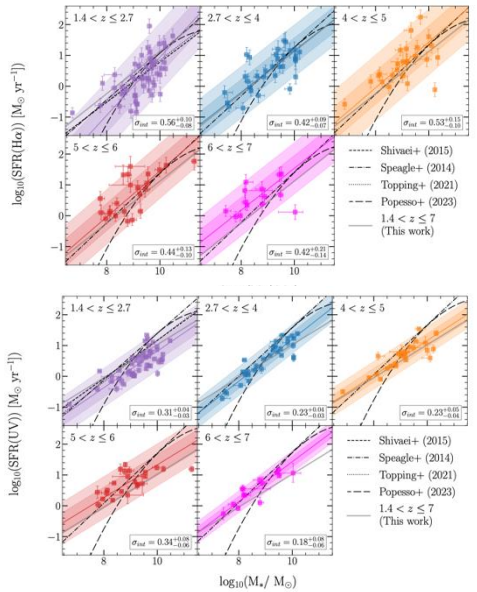

$$\log(\mathrm{SFR}) = m \times \log\left(\frac{\mathrm{M_*}}{10^{9.16}\mathrm{M_\odot}}\right) + b + \mathcal{N}(0, \sigma_{\mathrm{int}}^2)$$

estimate the best-fit parameters by using the Python Markov Chain Monte Carlo (MCMC) implementation **emcee**

SFR Indicator	Redshift Bin	m	b	σ_{int}	$\sigma_{\mathrm{int,low}}$ [a]	$\sigma_{\mathrm{int,high}}$ [b]	N
Hα	$1.4 < z \leq 7.0$	$0.69^{+0.07}_{-0.08}$	$0.56^{+0.05}_{-0.05}$	$0.53^{+0.05}_{-0.04}$	$0.57^{+0.05}_{-0.04}$	$0.59^{+0.04}_{-0.04}$	146
Hα	$1.4 < z \leq 2.7$	$0.95^{+0.15}_{-0.18}$	$0.16^{+0.09}_{-0.09}$	$0.56^{+0.10}_{-0.08}$	$0.89^{+0.33}_{-0.28}$	$0.58^{+0.06}_{-0.06}$	52
Hα	$2.7 < z \leq 4.0$	$0.67^{+0.10}_{-0.12}$	$0.59^{+0.09}_{-0.08}$	$0.42^{+0.09}_{-0.07}$	$0.45^{+0.07}_{-0.08}$	$0.44^{+0.07}_{-0.07}$	32
Hα	$4.0 < z \leq 5.0$	$0.74^{+0.15}_{-0.20}$	$0.81^{+0.12}_{-0.12}$	$0.54^{+0.15}_{-0.10}$	$0.26^{+0.09}_{-0.10}$	$0.74^{+0.11}_{-0.09}$	25
Hα	$5.0 < z \leq 6.0$	$0.75^{+0.13}_{-0.16}$	$0.83^{+0.12}_{-0.11}$	$0.44^{+0.13}_{-0.10}$	$0.51^{+0.08}_{-0.08}$	$0.32^{+0.12}_{-0.13}$	23
Hα	$6.0 < z \leq 7.0$	$0.69^{+0.13}_{-0.26}$	$0.97^{+0.20}_{-0.15}$	$0.42^{+0.21}_{-0.14}$	$0.26^{+0.10}_{-0.11}$	$0.62^{+0.11}_{-0.21}$	14
SED	$1.4 < z \leq 7.0$	$0.53^{+0.02}_{-0.04}$	$0.51^{+0.04}_{-0.04}$	$0.45^{+0.03}_{-0.03}$	$0.44^{+0.02}_{-0.02}$	$0.47^{+0.02}_{-0.02}$	146
SED	$1.4 < z \leq 2.7$	$0.62^{+0.09}_{-0.09}$	$0.23^{+0.06}_{-0.06}$	$0.39^{+0.05}_{-0.04}$	$0.34^{+0.03}_{-0.03}$	$0.39^{+0.02}_{-0.01}$	52
SED	$2.7 < z \leq 4.0$	$0.72^{+0.11}_{-0.14}$	$0.61^{+0.09}_{-0.09}$	$0.48^{+0.09}_{-0.07}$	$0.29^{+0.03}_{-0.03}$	$0.54^{+0.04}_{-0.04}$	32
SED	$4.0 < z \leq 5.0$	$0.55^{+0.08}_{-0.08}$	$0.59^{+0.10}_{-0.09}$	$0.44^{+0.10}_{-0.07}$	$0.27^{+0.03}_{-0.03}$	$0.55^{+0.07}_{-0.05}$	25
SED	$5.0 < z \leq 6.0$	$0.55^{+0.04}_{-0.09}$	$0.81^{+0.10}_{-0.10}$	$0.44^{+0.10}_{-0.07}$	$0.40^{+0.04}_{-0.03}$	$0.41^{+0.06}_{-0.05}$	23
SED	$6.0 < z \leq 7.0$	$0.63^{+0.09}_{-0.17}$	$0.90^{+0.14}_{-0.12}$	$0.36^{+0.15}_{-0.10}$	$0.36^{+0.07}_{-0.06}$	$0.08^{+0.11}_{-0.08}$	14
UV	$1.4 < z \leq 7.0$	$0.54^{+0.03}_{-0.04}$	$0.58^{+0.03}_{-0.03}$	$0.34^{+0.02}_{-0.02}$	$0.35^{+0.02}_{-0.01}$	$0.34^{+0.01}_{-0.01}$	145
UV	$1.4 < z \leq 2.7$	$0.59^{+0.07}_{-0.07}$	$0.32^{+0.05}_{-0.05}$	$0.31^{+0.04}_{-0.03}$	$0.24^{+0.02}_{-0.02}$	$0.33^{+0.01}_{-0.01}$	52
UV	$2.7 < z \leq 4.0$	$0.68^{+0.05}_{-0.06}$	$0.63^{+0.05}_{-0.05}$	$0.23^{+0.04}_{-0.03}$	$0.20^{+0.02}_{-0.02}$	$0.26^{+0.03}_{-0.03}$	31
UV	$4.0 < z \leq 5.0$	$0.56^{+0.06}_{-0.06}$	$0.68^{+0.05}_{-0.05}$	$0.23^{+0.05}_{-0.04}$	$0.16^{+0.02}_{-0.02}$	$0.30^{+0.04}_{-0.04}$	25
UV	$5.0 < z \leq 6.0$	$0.53^{+0.03}_{-0.05}$	$0.88^{+0.08}_{-0.07}$	$0.34^{+0.07}_{-0.06}$	$0.32^{+0.06}_{-0.04}$	$0.30^{+0.07}_{-0.07}$	23
UV	$6.0 < z \leq 7.0$	$0.64^{+0.08}_{-0.09}$	$0.88^{+0.08}_{-0.07}$	$0.18^{+0.08}_{-0.06}$	$0.22^{+0.05}_{-0.06}$	$0.08^{+0.04}_{-0.08}$	14

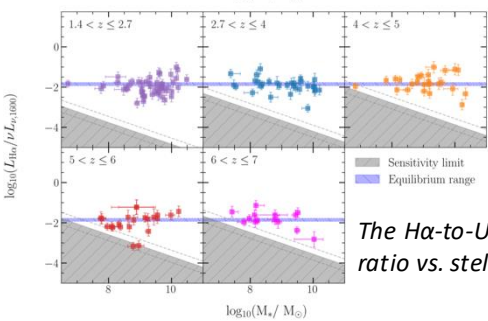

The Hα-to-UV luminosity ratio vs. stellar mass

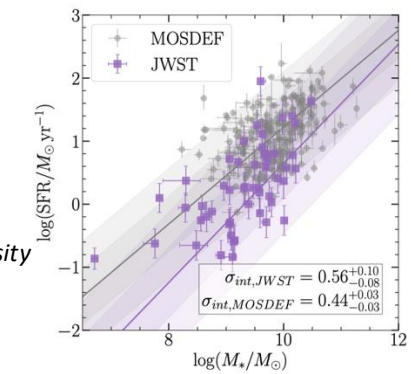

The Hα-based SFMS from JWST observations at $1.4 < z \leq 2.7$ (purple) and MOSDEF observations at $2.0 < z < 2.6$

Discussion:

1. SFR Intrinsic Scatter

The Hα-based SFMS is characterized by a larger intrinsic scatter than the UV-based SFMS by 0.21±0.05 dex
Not see any consistent mass dependence on intrinsic scatter from the low- to high-mass bins across redshift.

a) Comparison to theoretical works
Dominguez+2015 gasoline hydrodynamic simulations: consistent in UV, larger scatter in observation of Hα
Donnari+2019 IllustrisTNG simulations: observations exceeds the predictions in both
(The inability to resolve these processes the burstiness of SFHs in models)

b) Comparison to observational works
Tentatively observe a mass dependence comparing to MOSDEF sample ($10^{9.48} M_\odot$ vs. $10^{9.98} M_\odot$)
A larger, mass-complete spectroscopic sample is needed

2. The Hα-to-UV luminosity ratio

Hα and UV luminosities (Timescale: ~5 Myr and ~100 Myr)
Mehta+2023: the L(Hα)/L(UV) ratio reaches an equilibrium after ~100-200 Myr, reaching values the range of −1.93 and −1.78 (different metallicitiy).
Asada+2024: 60% of their galaxies deviate from a constant SFH by greater than 1σ.
This work: 29–52% of galaxies in the sample deviate from this ratio predicted for a constant SFH over a 100 Myr timespan
Decreasing star-formation (low Hα/UV ratio) and Rising star-formation (high Hα/UV ratio): galaxies at similar evolutionary stages have a mixture of both rising and falling SFHs

Redshift Bin	f_{eq}^a	f_{above}^b	f_{below}^c	$\sigma_{\mathrm{H\alpha/UV}}^d$
$1.4 < z \leq 2.7$	0.54	0.13	0.33	$0.3^{+0.05}_{-0.05}$
$2.7 < z \leq 4$	0.71	0.13	0.16	$0.3^{+0.07}_{-0.06}$
$4 < z \leq 5$	0.52	0.32	0.16	$0.36^{+0.09}_{-0.08}$
$5 < z \leq 6$	0.48	0.17	0.35	$0.46^{+0.1}_{-0.09}$
$6 < z \leq 7$	0.64	0.21	0.14	$0.29^{+0.13}_{-0.1}$